

Complex of rat transthyretin with tetraiodothyroacetic acid refined at 2.1 and 1.8 Å resolution[★]*

Tadeusz Muzioł¹, Vivian Cody², Joseph R. Luft², Walter Pangborn² and Andrzej Wojtczak¹ ✉

¹*Institute of Chemistry, Nicolaus Copernicus University, Toruń, Poland;* ²*Hauptman-Woodward Medical Research Institute, Inc., Buffalo, U.S.A.*

Received: 16 October, 2001; accepted: 3 December, 2001

Key words: rat transthyretin, tetraiodothyroacetic acid complex, crystal structure, multiple binding modes

The crystal structure of rat transthyretin (rTTR) complex with 3,5,3',5'-tetraiodothyroacetic acid (T4Ac) was determined at 1.8 Å resolution with low temperature synchrotron data collected at CHESS. The structure was refined to $R = 0.207$ and $R_{\text{free}} = 0.24$ with the use of 8–1.8 Å data. The additional 8000 reflections from the incomplete 2.1–1.8 data shell, included in the refinement, reduced the R_{free} index by 1.3%. Structure comparison with the model refined against the complete 8–2.1 Å data revealed no differences in the ligand orientation and the conformation of the polypeptide chain in the core regions. However, the high-resolution data included in the refinement improved the model in the flexible regions poorly defined with the lower resolution data. Also additional sixteen water molecules were found in the difference map calculated with the extended data. The structure revealed both forward and reverse binding of tetraiodothyroacetic acid in one binding site and two modes of forward ligand binding in the second site, with the phenolic iodine atoms occupying different sets of the halogen binding pockets.

Thyroxine (T4) and 3,5,3'-triiodothyronine (T3) are the main products secreted from the thyroid gland and their action influences oxygen metabolism and the biosynthesis of gly-

cerides and cholesterol [1, 2]. These hormones bind to the serum transport proteins thyroxine-binding globulin (TBG), transthyretin (TTR) and serum albumin, as well as to cellu-

[★]Presented at the XXXVII Convention of the Polish Biochemical Society, Toruń, Poland, September, 10–14, 2001.

*The research was partly supported by KBN 6/P04A/032/11 and GUMK 319-Ch grants (AW) and NIH FIRCA Fogarty TW00226 (VC).

✉To whom correspondence should be addressed: Andrzej Wojtczak, Institute of Chemistry, Nicolaus Copernicus University, Gagarina 7, 87-100 Toruń, Poland; tel. (48 56) 611 4506; fax: (48 56) 654 2477; e-mail: awojt@chem.uni.torun.pl

Abbreviations: TBG, thyroxine-binding globulin; T4, thyroxine; T4Ac, 3,5,3',5'-tetraiodothyroacetic acid; T3, 3,5,3'-triiodothyronine; TTR, transthyretin.

lar receptors [1]. Relative binding data for thyroid hormones and their metabolites revealed that specific structural characteristics enhance optimal binding to these proteins [1]. Although T4 has the greatest binding affinity for TBG, it is the acid metabolites that exhibit the greatest binding to TTR. For example, the metabolite 3,5,3',5'-tetraiodothyroacetic acid (T4Ac) has 2.8 times the affinity of T4 for TTR. In man, about 20% of T4 is transported as a TTR-T4 complex. The most important moieties of the ligands with high affinity to TTR are the carboxylic group and the iodinated phenolic ring [1]. The α -amino acids revealed affinity to TTR lower than their des-amino analogs (Fig. 1).

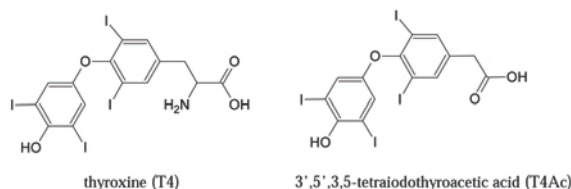


Figure 1. Schematic representation of thyroxine (T4) and tetraiodothyroacetic acid (T4Ac)

Transthyretin (TTR) is a homotetramer with molecular mass about 55-kDa (Fig. 2). Each subunit is a 127 amino-acid β -barrel, consisting of eight β -strands arranged in two β -sheets and a short α -helix [3–10]. Monomers forming a horizontal dimer AB are connected by hydrogen bonds along strands H and F. The central channel of the tetramer contains two independent binding sites [3], which differ in the ligand binding affinity. A negative cooperativity has been observed for the binding of T4 and other TTR ligands [7, 8, 11, 12].

Each binding domain of the tetramer contains three pocket regions P1–P3 that are responsible for halogen binding [5, 6]. The inner-most P3 pockets are polar. The hydrophobic P2 pockets are in the middle section of the binding site. The outer-most P1 pockets are positioned near the charged Lys-15 and Glu-54 in the vicinity of the channel entrance.

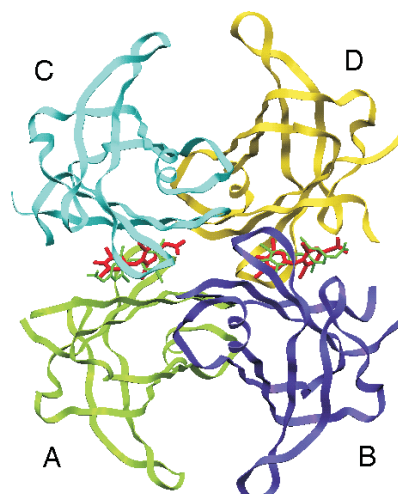


Figure 2. The rTTR-T4Ac complex.

The monomers constituting the asymmetric unit are labelled A to D. The ligand molecules bound in the two sites are also shown. Figure prepared with SETOR [25].

Human TTR crystals have orthorhombic P2₁2₁2 symmetry [3–8]. In the human TTR complexes, there is statistical disorder of the occupancy of the ligand that is a consequence of the twofold crystallographic symmetry of the channel not shared by the ligand molecules. On the other hand, rat TTR which shares 85% sequence homology with hTTR, forms tetragonal crystals that contain the complete tetramer in the asymmetric unit [9, 10]. The crystallographic symmetry axes are not coincident with the channel axis in the rTTR structures, which enables the recognition of the specific ligand–protein interactions that are not biased by the statistical disorder of the ligand [10].

The aim of this research was to compare the influence of partial data on refinement by comparison of refinement statistics for complete data to 2.1 Å resolution with incomplete data to 1.8 Å resolution.

EXPERIMENTAL

Rat TTR was obtained from rat serum (Pel-Frez; Rogers, AZ) by affinity chromatog-

raphy on a retinol-binding protein column. Rat TTR was incubated for 24 h with an excess of T4Ac ligand, then crystallized by the hanging drop vapor diffusion method. A detailed description of the crystallization conditions is published elsewhere [13]. The diffraction data were collected at CHESS A2 beamline at 100 K. The T4Ac-rTTR complex crystals have tetragonal $P4_32_12$ symmetry and are isomorphous with apo rTTR [9]. Therefore the structure of apo rTTR was used for initial phasing. The parameters and topology for the ligand were defined based on the small molecular structure of T4Ac [14] and quantum-chemical calculations with the AM1 method [15]. The parameters are based on the anionic form of the ligand which is consistent with the crystallization conditions (pH = 5.0). An analysis of reflection file with DATAMAN [16] revealed that effective resolution is 2.04 Å for reflections with $I/\sigma(I) > 3$, although the experimental resolution limit was 1.8 Å. The intensity, completeness and R_{merge} index in different resolution shells are presented in Table 1.

Data analysis has shown that R_{merge} increased to 0.104 for the 2.13–2.06 Å shell, and to 0.351 for the highest shell, whereas for all reflections it was only 0.048. The completeness of the highest 2.1–1.8 Å shell was only 42.9% (28% for 1.84–1.8 Å), whereas for the 2.13–2.06 Å shell and for all data it was 59% and 70.2%, respectively. The intensity of the reflections also decreased for the highest shell (Table 1). An analysis performed in DATAMAN revealed that the mean $F/\sigma(F)$ for reflections in the 2.1–1.8 Å resolution shell is 12.7 whereas for all reflections it is 37.2. The incompleteness of the diffraction data might have a great impact on final results [17–19]. Therefore we decided to refine the structure with the resolution range extended to 8–1.8 Å and to compare the obtained result with the structure refined with the 8–2.1 Å complete data. The refinement process was carried out with the use of the X-PLOR [20] and CNS [21] programs and the model was verified with O [22]. The structure has been deposited in the Protein Data Bank, the PDB code is 1KGI.

Table 1. R_{merge} , data completeness and the intensity/sigma ratio in different resolution shells

Resolution	R_{merge}	Completeness (%)	$I/\sigma(I) < 1$ (%)	$I/\sigma(I) < 3$ (%)	$I/\sigma(I) > 20$ (%)
46.7–4.44	0.048	86.7	0.5	0.9	74.9
4.44–3.52	0.041	90.4	0.3	0.8	77.3
3.52–3.08	0.042	94	1.2	2.5	73.8
3.08–2.80	0.048	93.9	2.0	3.5	64.9
2.80–2.60	0.053	93.3	2.9	5.7	53.3
2.60–2.44	0.060	92.9	3.5	6.7	40.7
2.44–2.32	0.067	92.4	4.0	9.0	30.3
2.32–2.22	0.069	82.3	4.0	9.2	14.8
2.22–2.13	0.073	67.1	4.7	9.9	6.3
2.13–2.06	0.104	59	4.8	11.1	3.1
2.06–2.00	0.124	52.6	5.9	12.5	1.6
2.00–1.94	0.157	45.8	6.9	13.9	0.6
1.94–1.89	0.193	36.7	8.4	15.7	0.3
1.89–1.84	0.281	32.3	9.0	16.8	0.0
1.84–1.80	0.351	28	9.4	18.5	0.0
All	0.048	70.2	4.4	9.0	30.1

RESULTS AND DISCUSSION

The main goal of this paper was to verify the importance of high resolution shells for positioning of both the ligand and the flexible fragments of the structure. The extension of the resolution range does not change the R value, but results in lowering the R_{free} index value, indicating an improvement of the final model (Table 2). These results suggest that addition

tional error has been introduced into the model and the ligand position was not affected. However, the ligand position was correctly defined by the lower resolution data alone. A further discussion of the ligand position will be carried out only for the final model (resolution 8–1.8 Å). The rms difference between the complex structures refined to 2.1 and to 1.8 Å, calculated with LSQMAN [23] for 432 C α positions of residues 10–98 and

Table 2. Results of data collection and refinement processes

Space group	P4 ₃ 2 ₁ 2	
Cell parameters (Å)	a = b = 81.510 c = 160.235	
Resolution range (Å) – measured	46.7–1.8	
Resolution range (Å) used in refinement	8–2.1	8–1.8
Reflections used	25471	29735
Reflections in test set	1063	2620
% of possible reflections used	83.9	64.5
R factor	0.208	0.207
R_{free}	0.253	0.240
Protein atoms	3737	3737
Water molecules	265	281
B factor (Wilson stat.) (Å ²)	23.2	23.1
B factor (average) (Å ²)	30.51	34.71
B factor (protein) (Å ²)	30.27	34.45
B factor (water) (Å ²)	33.27	37.79
rms deviations from ideality:		
Bond distances (Å)	0.006	0.006
Angles (°)	1.219	1.198
Ramachandran plot statistics (%)		
Residues in most favored regions	368 (88.2)	367 (88.0)
Residues in additional allowed regions	47 (11.3)	48 (11.5)
Residues in generously allowed regions	2 (0.5)	2 (0.5)

of incomplete data with a higher R_{merge} index and lower intensity of reflections could be useful to the final refinement. The position of the ligand does not change after the use of incomplete 2.1–1.8 Å resolution data, despite the extensive refinement with the simulated annealing protocol (Figs. 3, 4). This indicates that the partial data are of good quality, no addi-

105–123, is only 0.073 Å. The shape and size of the channel remain unchanged. This result is confirmed by a multiple model Ramachandran plot (Fig. 5). The largest differences were found for Gln-126 and Gly-701 positioned in flexible regions. An analysis of the χ_1 and χ_2 torsion angles revealed significant changes for amino acids of the flexible fragments at

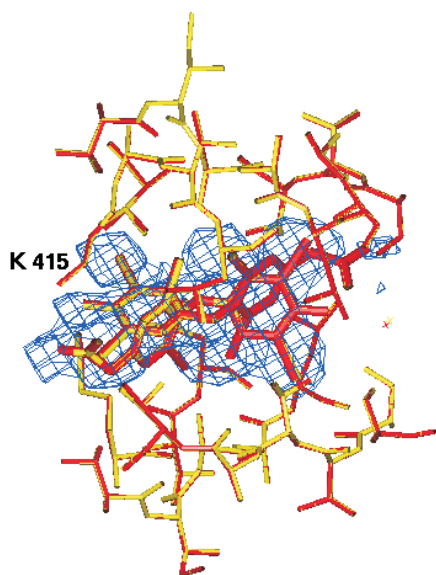


Figure 3. Comparison of the complex structure refined to 1.8 Å resolution (red) and 2.1 Å resolution (yellow) in the A/C site.

The σ_A -weighted SA omit map contoured at 1σ is colored blue.

the N- and C-termini, as well as loops 56–66 and 98–105 (Fig. 6). The extension of the data resolution permitted 16 new water molecules to be found in the difference maps. A comparison of the solvent structure in both models re-

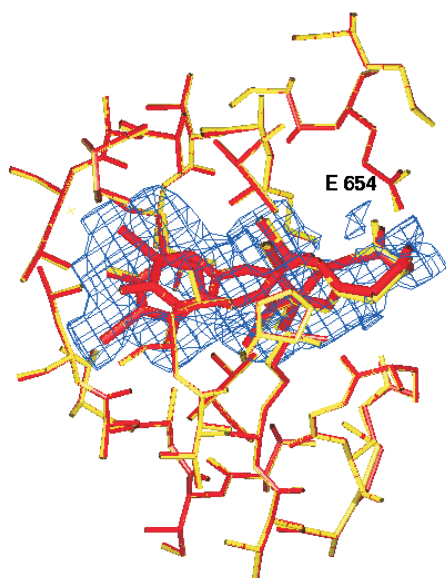


Figure 4. Comparison of the rTTR–T4Ac complex structures refined to 1.8 Å resolution (red) and 2.1 Å resolution (yellow) in the B/D site.

The σ_A -weighted SA omit map contoured at 1σ is colored blue.

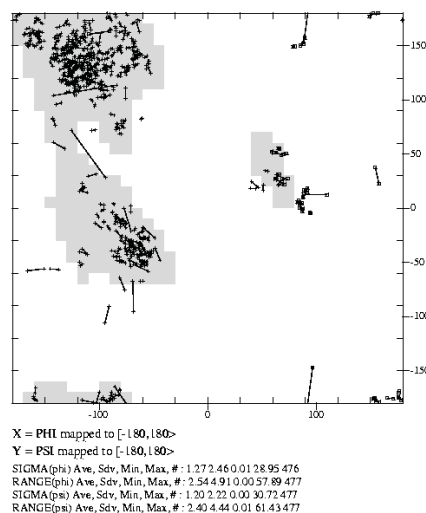


Figure 5. Multiple model Ramachandran plot reveals high similarity of the 2.1 Å and 1.8 Å models of the rTTR–T4Ac complex.

vealed that 249 water molecules do not move by more than 0.7 Å, while the average shift is 0.17 Å.

The rTTR homotetramer contains two binding sites in the protein channel. The total ligand occupancy found in the A/C (0.38) is higher than in the B/D site (0.28). An analysis of electron density maps revealed multiple binding modes in both binding sites. The final model contains two alternative orientations in

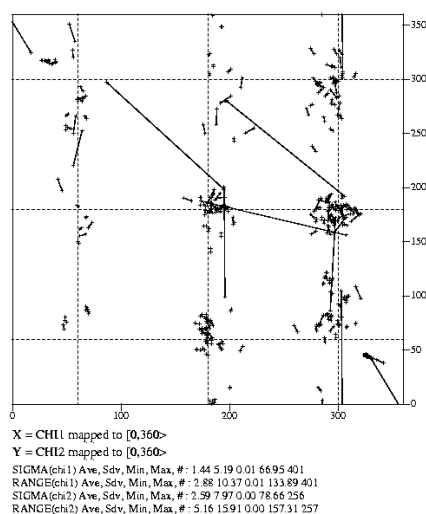


Figure 6. Differential plot of the side chain conformation reveals only small changes caused by the incomplete 2.1–1.8 Å resolution data.

the A/C site with occupancies 0.20 and 0.18. The ligand in the major population is bound in the reverse mode. In this mode the phenyl ring of T4Ac is bound at the channel entrance and the acetic moiety in the inner-most P3 pocket. Such an orientation has been postulated [3] but never observed for any other T4 analogue. Therefore, the T4Ac complexes with TTR are first structures reported with the binding in such orientation [13]. In the reverse ligand orientation main interactions are formed inside the channel with Ser-517 and two water molecules at the interface between the two binding sites. In this orientation the ligand molecule penetrates the tetramer interface and interacts with Ser-715 of the second binding site. The tyrosyl iodine atoms are positioned in the P2 pockets. Polar interactions are formed at the channel entrance between O4' and I5' of the ligand and Lys-15 and Thr-106, some of them mediated by water molecules. These interactions reveal the significance of solvent molecules for effective ligand binding.

The forward orientation of the ligand with the lower occupancy was also detected in the A/C site. In this orientation the phenolic iodine substituents are bound in both the P3 and P3' pockets. The phenolic iodine atoms interact with Ser-117, Ser-517, Thr-519 and a water molecule. A similar orientation of the phenolic ring was reported for thyroxine in rTTR [10] and monoclinic hTTR [24] complexes. In this orientation the ligand also interacts with Lys-415 in the P1' pocket.

In the B/D site electron density maps revealed two P3/P2' ligand orientations related by non-crystallographic twofold axis coincident with the channel axis coupled with a shift by about 1 Å along the channel axis. The water molecule bound in the P3' pocket may influence the binding position of the two ligands in this site. This water molecule mediates an interaction between Ser-717 and the ligand. The analysis revealed that the binding interactions of T4Ac in the P3/P2' mode are weaker than those in the reverse mode or in the for-

ward orientation found in the A/C site. Neither of the ligand molecules bound in the B/D site interacts directly with Lys-215 or Lys-615. However, Glu-654 is involved in interactions with the ligand carboxylic groups (T4Ac-328 O9...Glu-654 OE2). One possible explanation for such observation is that one of these carboxyl groups is protonated.

CONCLUSIONS

A refinement of the rTTR-T4Ac complex structure with data extended to 1.8 Å resolution is reported. Due to the lack of the twofold symmetry of the binding channel, the ligand-protein interactions were analyzed without the bias caused by the statistical disorder of the ligand observed in the human TTR complex. The T4Ac ligand revealed different orientations in both binding sites. The reverse binding of T4Ac, found in the A/C site, is unique among L-thyronine analogues. The analysis of interactions and electron density maps revealed that this is the most effective binding mode of T4Ac in TTR channel. The comparison of the refinement results for different resolution ranges revealed that the extension of the resolution by including the incomplete high resolution reflections shell has improved the structure quality, which is reflected in the R_{free} index, whereas the R index is not sensitive to this extension. The comparison of both models revealed that, with the partial data included, the polypeptide chain in the core regions is not changed significantly. The model improvement was observed for the flexible regions of the protein with the weak electron density maps calculated from the complete 8–2.1 Å resolution data. Also the orientation of the ligand was not changed by the incomplete data. This indicates that even partial high resolution data are useful for improving the quality of the model, although the ligand position could be defined correctly with the use of the lower resolution data alone.

REFERENCES

1. Jorgensen, E.C. (1978) Thyroid hormones and analogues. II. Structure-activity relationships; in *Hormonal Proteins and Peptides* (Li, C.H., ed.) vol. 6, pp. 108-204, Academic Press, New York.
2. Hutinec, A., Ziogas, A., & Rieker, A. (1996) Non-natural phenolic acids. Synthesis and application in peptide chemistry. *Amino Acids* 1996, 345-366.
3. De la Paz, P., Burridge, J.M., Oatley, S.J. & Blake, C.C.F. (1992) Multiple modes of binding of thyroid hormones and other iodothyronines to human plasma transthyretin; in *The Design of Drugs to Macromolecular Targets* (Beddell, C.R., ed.) pp. 120-172, John Wiley & Sons Ltd.
4. Hamilton, J.A., Steinrauf, L.K., Braden, B.C., Liepnieks, J., Benson, M.D., Holmgren, G., Sandgren, O. & Steen, L. (1993) The X-ray crystal structure refinements of normal human transthyretin and the amyloidogenic Val30Met variant to 1.7 Å resolution. *J. Biol. Chem.* **268**, 2416-2424.
5. Blake, C.C.F., Geisow, M.J., Oatley, S.J., Rerat, B., & Rerat, C. (1978) Structure of prealbumin: Secondary, tertiary and quaternary interactions determined by Fourier refinement at 1.8 Å. *J. Mol. Biol.* **121**, 339-356.
6. Wojtczak, A., Cody, V., Luft, J. & Pangborn, W. (1996) Structures of human transthyretin complexed with thyroxine at 2.0 Å resolution and 3',5'-dinitro-*N*-acetyl-L-thyronine at 2.2 Å resolution. *Acta Crystallogr. D* **52**, 758-765.
7. Peterson, S.A., Klabunde, T., Lashuel, H.A., Purkey, H., Sacchettini, J.C. & Kelly, J.W. (1998) Inhibiting transthyretin conformational changes that lead to amyloid fibril formation. *Proc. Natl. Acad. Sci. U.S.A.* **95**, 12956-12960.
8. Petrassi, H.M., Klabunde, T., Sacchettini, J. & Kelly, J.W. (2000) Structure-based design of *N*-phenyl phenoxazine transthyretin amyloid fibril inhibitors. *J. Am. Chem. Soc.* **122**, 2178-2192.
9. Wojtczak, A. (1997) Crystal structure of rat transthyretin at 2.5 Å resolution: First report on a unique tetrameric structure. *Acta Biochim. Polon.* **44**, 505-518.
10. Wojtczak, A., Cody, V., Luft, J. & Pangborn, W. (2001) Structure of rat transthyretin (rTTR) complex with thyroxine at 2.5 Å resolution: First non-biased insight into thyroxine binding reveals different hormone orientation in two binding sites. *Acta Crystallogr. D* **57**, 1061-1070.
11. Pages, R.A., Robbins, J. & Edelhofer, H. (1973) Binding of thyroxine and thyroxine analogs to human serum prealbumin. *Biochemistry* **12**, 2773-2779.
12. Ferguson, R.N., Edelhofer, H., Saroff, H.A. & Robbins, J. (1975) Negative cooperativity in the binding of thyroxine to human serum prealbumin. *Biochemistry* **14**, 282-289.
13. Wojtczak, A., Neumann, P., Muzioł, T. & Cody, V. (2001) Novel binding mode of tetraiodothyroacetic acid in transthyretin. *Acta Crystallogr. D*. Submitted.
14. Cody, V., Hazel, J., Langs, D.A. & Duax, W.L. (1977) Molecular structure of thyroxine analogs. Crystal structure of 3,3',5-triiodothyroacetic and 3,5,3',5'-tetraiodothyroacetic acid *N*-diethanolamine (1:1) complexes. *J. Med. Chem.* **20**, 1628-1631.
15. Nowak, W. & Wojtczak, A. (1997) Quantum chemical modelling of thyroid hormone analogues. *J. Mol. Struct. (Theochem)* **419**, 121-131.
16. Kleywegt, G.J. & Jones, T.A. (1996) xdlMAPMAN and xdlDATAMAN - programs for reformatting, analysis and manipulations of biomacromolecular electron-density maps and

- reflections data sets. *Acta Crystallogr.* **D52**, 826–828.
- 17.** Guo, D.Y., Blessing, R.H. & Langs, D.A. (2000) On “globbicity” of low-resolution protein structures. *Acta Crystallogr.* **D56**, 451–457.
- 18.** Kleywegt, G.J. (2000) Validation of protein crystal structures. *Acta Crystallogr.* **D56**, 249–265.
- 19.** Dodson, E., Kleywegt, G.J. & Wilson, K. (1996) Report of a workshop on the use of statistical validators in protein X-ray crystallography. *Acta Crystallogr.* **D52**, 228–234.
- 20.** Brunger, A. (1992) *XPLOR Version 3.1. A System for X-ray Crystallography and NMR*. Yale University Press, New Haven.
- 21.** Brünger, A.T., Adams, P.D., Clore, G.M., DeLano, W.L., Gros, P., Grosse-Kunstleve, R.W., Jiang, J.-S., Kuszewski, J., Nilges, M., Pannu, N.S., Read, R.J., Rice, L.M., Simonson, T. & Warren, G.L. (1998) Crystallography & NMR system: A new software suite for macromolecular structure determination. *Acta Crystallogr.* **D54**, 905–921.
- 22.** Jones, T.A., Zou, J.Y., Cowan, S.W. & Kjeldgaard, M. (1991) Improved methods for building proteins models in electron density maps and the location of errors in these models. *Acta Crystallogr.* **A47**, 110–119.
- 23.** Kleywegt, G.J. (1996) Use of non-crystallographic symmetry in protein structure refinement. *Acta Crystallogr.* **D52**, 842–857.
- 24.** Wojtczak, A., Neumann, P. & Cody, V. (2001) Structure of a new polymorphic monoclinic form of human transthyretin at 3 Å resolution reveals a mixed complex between unliganded and T4-bound tetramers of TTR. *Acta Crystallogr.* **D57**, 957–967.
- 25.** Evans, S.V. (1993) SETOR: Hardware lighted three-dimensional solid model representations of macromolecules. *J. Mol. Graphics* **11**, 134–138.